https://doi.org/10.5194/egusphere-2025-2438
Preprint. Discussion started: 16 June 2025


# Non-Stationary Dynamics of Compound Climate Extremes: A WRF-CMIP6-GAMLSS Framework for Risk Reassessment in Southeastern China

Yinchi Zhang[1, 2, 3], Wanling Xu[4], Chao Deng[5], Shao Sun[6], Miaomiao Ma[7], Jianhui Wei[8], Ying Chen[1, 2, 3, 9], Harald Kunstmann[8], Lu Gao[1, 2, 3, 9*]

[1]*Key Laboratory for Humid Subtropical Eco-geographical Processes of the Ministry of Education, Fujian Normal University, Fuzhou, 350117, China*

[2]*Institute of Geography, Fujian Normal University, Fuzhou, 350117, China*

[3]*School of Geographical Science, Fujian Normal University, Fuzhou, 350117, China*

[4]*School of Ocean and Earth Science, Tongji University, Shanghai, 200092, China*

[5]*School of Geography and Ecotourism, Southwest Forestry University, Kunming 650224, China*

[6]*State Key Laboratory of Severe Weather, Chinese Academy of Meteorological Sciences, Beijing 100081, China*

[7]*China Institute of Water Resources and Hydropower Research, Beijing, 100038, China*

[8]*Institute of Meteorology and Climate Research (IMKIFU), Karlsruhe Institute of Technology, Campus Alpin, Garmisch-Partenkirchen, Germany*

[9]*Fujian Provincial Engineering Research Center for Monitoring and Accessing Terrestrial Disasters, Fujian Normal University, Fuzhou, 350117, China*

***Corresponding Author: Lu Gao, l.gao@foxmail.com**

https://doi.org/10.5194/egusphere-2025-2438
Preprint. Discussion started: 16 June 2025


**Abstract**

Understanding future changes in compound climate extremes (CCEs) is critical for climate risk assessment. However, existing research have relied on stationary assumptions, overlooking the dynamic evolution of CCEs under non-stationary climate change. Therefore, based on an enhanced Generalized Additive Models for Location, Scale, and Shape (GAMLSS), this study provides novel perspectives into the non-stationary characteristics of hot-wet (HW), hot-dry (HD), cold-wet (CW), and cold-dry (CD) extremes under future climate scenarios, focusing on the Minjiang River Basin (MRB), located in Southeast China. The high-resolution dataset employed for CCEs detection is generated through dynamical downscaling of a bias-corrected CMIP6 dataset, utilizing the Weather Research and Forecasting (WRF) model. The results show that (1) CCEs increase significantly at a rate of 3.55d/10a under the SSP5-8.5 scenario, with hot extremes (HW and HD) playing a dominant role. The spatial distribution exhibits a distinct west to east increasing gradient, peaking in the MRB downstream areas. (2) Under the SSP5-8.5 scenario, CCEs exhibit a marked transition from stationary to non-stationary characteristics, with non-stationarity detected in 95.20% of grid cells. Mean warming, not variability, served as the dominant factor behind this transition, explaining 80.81% of the changes. (3) The non-stationary results demonstrate that the severity and recurrence risks of CCEs are systematically underestimated. Most CCEs (except for CD) exhibit increasing recurrence risks under the SSP5-8.5 scenario, with a trend of 3.12d/10a in the 100-year return period, showing a stronger increase. This study emphasizes the necessity of updating the risk changes of CCEs under a non-stationary framework.

**Keywords** compound climate extremes, non-stationarity, GAMLSS, dynamical downscaling, WRF

https://doi.org/10.5194/egusphere-2025-2438
Preprint. Discussion started: 16 June 2025


## 1 Introduction

Global warming is leading to more frequent and intense compound climate extremes (CCEs) (Sauter et al., 2023; Liu et al., 2024; Zhang et al., 2024; You et al., 2025). CCEs have posed severe threats to global social, economic, and ecological systems, with impacts that surpass those of individual extremes in both range and severity (Mukherjee et al., 2023; Zeng et al., 2024; Miao et al., 2024). For example, the Yangtze River Basin in China experienced unprecedented compound hot-dry extremes in August 2022, characterized by record-breaking heatwaves and severe droughts, which directly affected over 50 million people (Jia et al., 2025). The Sixth Intergovernmental Panel on Climate Change (IPCC) report indicated that the probability and intensity of future CCEs are projected to increase (IPCC, 2021). Therefore, a systematic assessment of the future evolution of CCEs is critical for mitigating socio-economic risks and optimizing climate adaptation strategies.

Traditional extreme event analyses rely on stationarity assumptions, presuming that the probability and distributional parameters of climate variables are constant (Sun et al., 2018; Nerantzaki et al., 2023). However, driven by synergistic effects of global warming and anthropogenic forcing, extremes exhibit significant shifts in distributional characteristics (Gao et al., 2018). Therefore, traditional models are not suitable for evaluating extreme changes in the changing environment. To capture these changes, many studies have applied the Generalized Additive Models for Location, Scale, and Shape (GAMLSS) (Rigby and Stasinopoulos 2005) to address non-stationary problems in hydrological and meteorological extremes, enabling updated risk analysis of evolving climate extremes (Lei et al., 2021; Shao et al., 2022; Jin et al., 2023; Li et al., 2024). However, existing non-stationary analyses only focus on individual extremes, and the potential non-stationarity of CCEs has not been established. The comprehensive assessment of future changes in CCEs recurrence risk within a non-stationary framework is also lacking.

The Coupled Model Intercomparison Project Phase 6 (CMIP6) dataset is widely used in climate change research, providing critical predictive understanding of forthcoming climate changes (Singh et al., 2023; Wu et al., 2024; Zhang et al., 2024; Yuan et al., 2024; Feng et al., 2025). While the CMIP6 dataset is applicable for global or large-scale studies, its relatively coarse spatial resolution poses limitations for local-scale investigations (Kim et al., 2020; Abdelmoaty et al., 2021; Zhang et al., 2024). To overcome this constraint, dynamical downscaling, which utilizes nested

https://doi.org/10.5194/egusphere-2025-2438
Preprint. Discussion started: 16 June 2025


high-resolution regional climate models (RCMs), provides a critical technical pathway to investigate climate response mechanisms at fine-scales (Tapiador et al., 2020; Rahimi et al., 2024). As an advanced convection-permitting atmospheric modeling system, the WRF model significantly enhances the simulation capability for meteorological processes at 1-10 km scales through its fully compressible, non-hydrostatic dynamic core framework (Talbot et al., 2012). Current WRF-based studies on CCEs predominantly rely on historical reanalysis data, focusing on attribution and simulation verification of past events (Zhang et al., 2025; Saini and Rohtash, 2025; Deng et al., 2025). Nevertheless, accurately projecting the evolving trends of future CCEs is crucial for improving localized disaster resilience and enhancing water security.

In this study, we develop an innovative non-stationary framework for CCE projection through dynamical downscaling of the bias-corrected CMIP6 (CMIP6bc) data, assessing recurrence risk evolution during 2025-2065. We focus on the Minjiang River Basin (MRB), a subtropical monsoon-dominated basin of southeastern China, where complex interactions between topography and climate give rise to high-intensity compound hydroclimatic extremes. The analysis proceeds as follows (Fig. 1): Supplement Section S1 presents the validation of CMIP6bc applicability. Section 3.1 characterizes the spatio-temporal patterns of CCEs under both a middle-of-the-road scenario (SSP2-4.5) and a high-emissions scenario (SSP5-8.5). The non-stationarity detection of CCEs is described in Section 3.2. The recurrence risk changes in CCEs under non-stationary conditions is evaluated in Section 3.3. The work establishes a scientific basis for addressing the environmental and climatic challenges posed by CCEs, thereby contributing to effective strategies for regional sustainability and climate resilience.

https://doi.org/10.5194/egusphere-2025-2438
Preprint. Discussion started: 16 June 2025


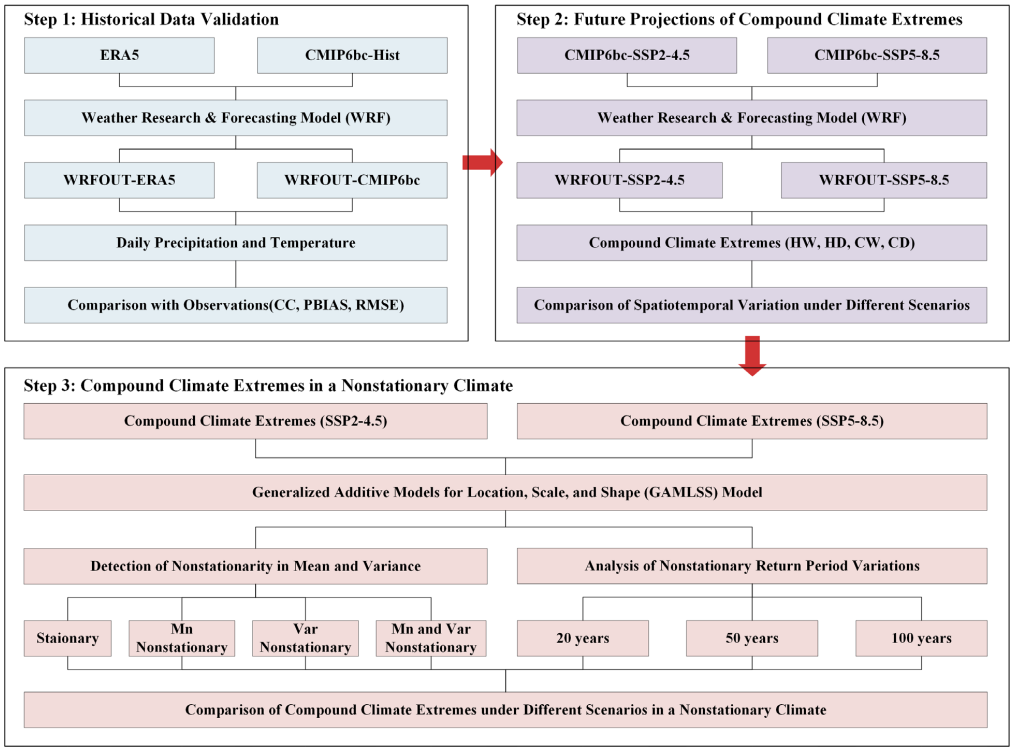


Fig. 1. Flowchart of CCEs projection in a non-stationary framework.

https://doi.org/10.5194/egusphere-2025-2438
Preprint. Discussion started: 16 June 2025


## 2 Study region, methods and data

### 2.1 Study region

The MRB is a complex topographic basin in southeastern coastal China (Fig. 2a). The Minjiang River, the main stream of the basin, drains an area of 60,992 km²–accounting for nearly half Fujian Province's territory. Encompassing three principal tributaries (Jianxi, Futunxi, and Shaxi rivers), the MRB experiences a subtropical monsoon climate characterized by 1700 mm mean annual precipitation and 18°C mean temperature. (Zheng et al., 2023). The basin displays spatio-temporal heterogeneity in precipitation, with flood seasons from April to September that often accompany CCEs.

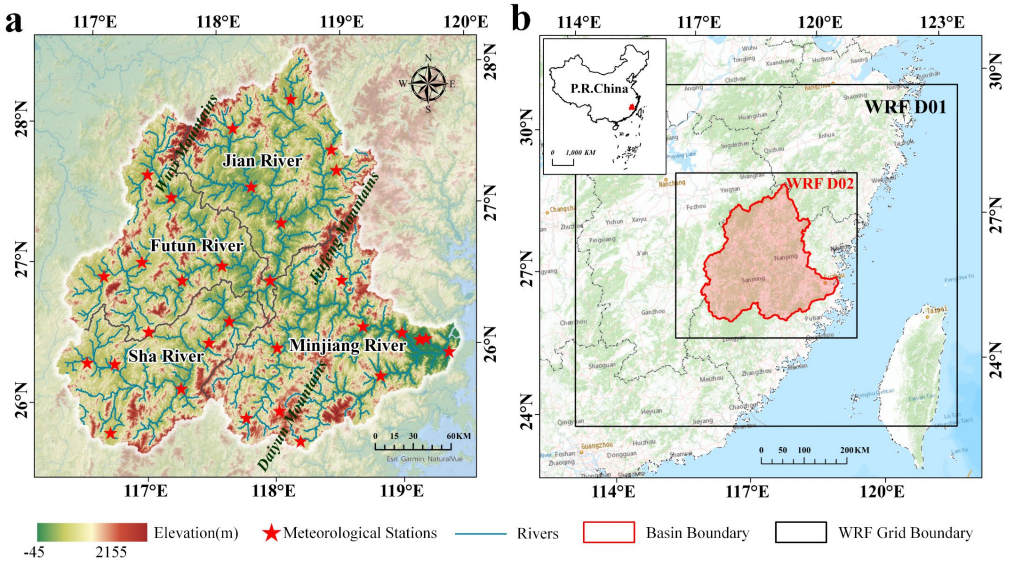


Fig. 2. Study area and model configuration. (a) Topographic features of the MRB (m) and (b) Model configuration with 9-km (D01) and 3-km (D02) nested domains (Zhang et al., 2025). Basemap source: © Esri, https://services.arcgisonline.com

https://doi.org/10.5194/egusphere-2025-2438
Preprint. Discussion started: 16 June 2025


## 2.2 Data

Fujian Provincial Meteorological Bureau provided daily precipitation and temperature records from its 30 monitoring stations. Obtained from the Science Data Bank, the CMIP6bc dataset serves as the foundation for this investigation (Xu et al., 2021, https://www.scidb.cn), which is constructed using the ERA5. This dataset incorporates an 18-model CMIP6 ensemble mean, maintaining both climatological mean and interannual variability statistics while preserving nonlinear temporal trends. Compared with original CMIP6 data, CMIP6bc demonstrates superior performance in extreme event simulation. The dataset used in this study covers the historical period (2005–2014) and future scenarios under SSP2-4.5 and SSP5-8.5 (2025–2065). Moreover, the ERA5, as a widely recognized forcing dataset, was used as a reference to evaluate the performance of historical simulations (Arnault et al., 2021; Jiang et al., 2021; Varga and Breuer, 2022; Shang et al., 2022).

## 2.3 Definition of CCEs

This study considers four types of CCEs: hot-wet events (HW), hot-dry events (HD), cold-wet events (CW) and cold-dry events (CD). We adopt the widely used thresholds (the 90th and 10th percentiles) to identify CCEs (Croitoru et al., 2016; Song et al., 2019; Patel et al., 2024). We first extract daily precipitation (>0.1 mm) and temperature data for each grid during 2025-2065, defining the 90th and 10th percentiles as thresholds to identify hot/cold and wet/dry extremes, respectively. Specifically, we define extreme temperature events as occurring when daily temperatures are higher (hot extremes) or lower (cold extremes) than the threshold. Wet events are characterized by rainfall surpassing the threshold (90th), while dry events are characterized by seven consecutive days without rainfall.

https://doi.org/10.5194/egusphere-2025-2438
Preprint. Discussion started: 16 June 2025


## 2.4 Model and experimental design

### 2.4.1 WRF model setup

This research utilizes the WRF Version 4.3 with two-domain nested configuration, featuring grid spacings of 9 km and 3 km (Fig. 2b). Table 1 summarizes the optimal physics parameterization schemes selected through our comprehensive sensitivity experiments (Lin et al., 2023; Zhang et al., 2025). At sufficiently high model resolutions, deep convective processes can be explicitly resolved (Arakawa and Jung, 2011). Therefore, the cumulus parameterization scheme is deactivated in the inner domain (D02) to leverage convection-permitting capability. We first simulate daily precipitation and temperature over the MRB from January 1, 2005 to December 31, 2014, using both CMIP6bc and ERA5 forcing data. Subsequently, future projections from January 1, 2025 to December 31, 2065 are conducted using CMIP6bc under two climate projection scenarios.

Table 1 Settings for WRF model in this study.

| WRF model setup overview | | Parameterization scheme settings | |
|---|---|---|---|
| Forcing data | CMIP6bc, ERA5 | Microphysics | Purdue Lin (Chen and Sun, 2002) |
| Centre | 118.02E°, 26.83N° | Cumulus convection | New Tiedtke (Zhang et al., 2011) |
| Grid | 100×90, 142×130 | Longwave radiation | RRTMG (Mlawer et al., 1997) |
| Resolution | 9km, 3km | Shortwave radiation | Dudhia (Dudhia, 1989) |
| E_vert | 45 | Boundary layer | YSU (Hong et al., 2006) |
| Spin-up time | 7 days | Land surface | Noah-MP (Niu et al., 2011) |

### 2.4.2 GAMLSS model

GAMLSS is a flexible statistical model used for analyzing distributions with non-stationary characteristics (Rigby and Stasinopoulos, 2005). It extends the traditional generalized linear models (GLMs) and generalized additive models (GAMs) by introducing joint modeling of all distribution parameters (location, scale, and shape). Unlike traditional regression models, GAMLSS effectively characterizes both linear and nonlinear dependencies linking predictors to response variables. (D. M. Stasinopoulos and Rigby, 2007).

This study employs the semi-parametric GAMLSS, which accommodates parametric terms, nonparametric smooth functions, and random effects within a unified modeling structure (Gao et al., 2018). Consider $z$ independent samples $y_i (i = 1, \dots, z)$ following a distribution $F_y(y_i \theta_i)$, where the parameter vector $\theta_{iT} = (\theta_{i1}, \theta_{i2}, \dots, \theta_{ik})$ contains $k$ components representing location (Mn), scale (Var), and shape (skewness and kurtosis), with $k$ normally not exceeding 4. Model

https://doi.org/10.5194/egusphere-2025-2438
Preprint. Discussion started: 16 June 2025


selection is performed using Akaike's Information Criterion (AIC) (Akaike, 1974), with the optimal configuration identified through minimum AIC values., and model fitting quality is assessed by the Filliben correlation coefficient (Filliben, 1975). The GAMLSS is formally defined as follows:

$$g_k(\theta_k) = \emptyset_k \beta_k + \sum_{j=1}^{j_k} h_{j_k}(x_{j_k})$$

where $k$ denotes the indicator of distribution parameters, $\theta_k$ is the distribution parameter vector, $\emptyset_k$ represents $n \times j_k$ matrix of covariate variables, $\beta_k$ is the coefficient vector of length $j_k$. $g_k(\cdot)$ is the link function connecting distribution parameter to linear predictor. $h_{j_k}(\cdot)$ defines how the distribution parameter varies with covariate variable $x_{j_k}$. To assess changes in CCE recurrence risk across the MRB, we fit non-stationary GAMLSS models with two parameters (mean, variance) and four parameters (mean, variance, skewness, kurtosis) at each grid point, selecting the optimal model for subsequent analysis. Supplement Table S1 enumerates all distribution functions implemented in our study. The R code for implementing GAMLSS model can be accessed at https://github.com/gamlss-dev/gamlss.

https://doi.org/10.5194/egusphere-2025-2438
Preprint. Discussion started: 16 June 2025


# 3 Results

## 3.1 Spatio-temporal patterns of CCEs under future scenarios

Figure 3 (a–j) illustrate the annual spatial distribution characteristics of CCEs in the MRB during 2025–2065. Overall, total CCEs are higher under the SSP5-8.5 scenario (45.48 days) than under the SSP2-4.5 scenario (42.58 days). Specifically, dry extremes (HD and CD), dominate the MRB, while wet-related extremes (HW and CW) occur less frequently. Both hot extremes occur more frequently under SSP5-8.5 than SSP2-4.5, with HW increasing from 0.84 to 1.33 days and HD rising from 22.69 to 27.45 days. In contrast, cold extremes exhibit an opposite trend, with CW decreasing from 3.17 to 2.15 days and CD declining from 15.88 to 14.19 days.

Spatially, both scenarios exhibit similar patterns in CCEs, with the highest frequency occurring in downstream—especially HD and HW, Whereas HD showing a broader distribution, extending to the Futun River and Jian River Basins. Furthermore, CW and CD follow a distinct west-to-east increasing gradient, with highest values near the Jiufeng Mountains.

Temporally (Fig. 3 k–o), the CCEs differ significantly between two emission scenarios. Under high-emission SSP5-8.5, total CCEs increase markedly (3.55d/10a), whereas SSP2-4.5 projects stabilized frequencies. Hot extremes (HW and HD) increase more rapidly under SSP5-8.5, with nearly double rates than those under SSP2-4.5. In contrast, CD shows stronger declining trend under SSP2-4.5 scenario, with approximately 1.7 times than SSP5-8.5.

https://doi.org/10.5194/egusphere-2025-2438
Preprint. Discussion started: 16 June 2025


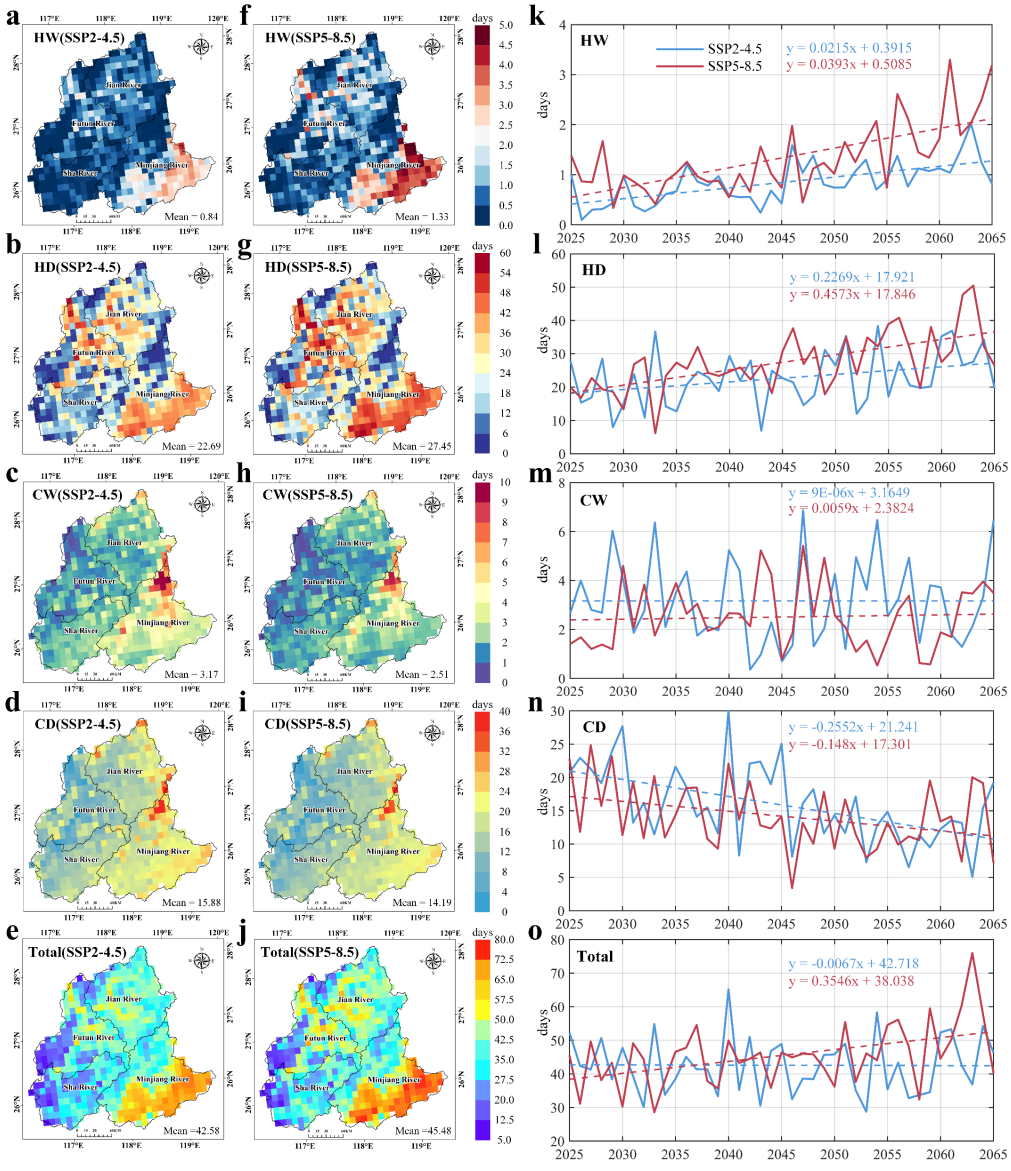


Fig. 3. Annual Spatio-temporal patterns of CCEs in the MRB from 2025 to 2065.

https://doi.org/10.5194/egusphere-2025-2438
Preprint. Discussion started: 16 June 2025


Having analyzed the annual changes in CCEs, we further identify the seasonal variations of CCEs. As shown in Fig. 4 (a–j), the spatial patterns of CCEs in summer generally align with annual distributions, except for HW, which are rarely observed during this season. Even so, a marked rise in HW under the SSP5-8.5 scenario is evident in the downstream MRB. In summary, total CCEs increase during summer under both scenarios, but with a significantly faster rate under SSP5-8.5 (2.26d/10a and 0.79d/10a). Moreover, the differences in warm events (HW, HD) between scenarios become more pronounced during summer than at the annual scale, while cold events (CW, CD) show consistent patterns (Fig. 4 k–o).

Winter, however, exhibits a contrasting spatial trend. Fig. 5 (a–j) indicate that CCEs primarily occur in the western MRB, particularly concentrated in the Futun River Basin, with higher frequencies under the SSP5-8.5 scenario (11.87 days and 11.51 days). This shift primarily results from the altered spatial distributions of warm extremes (HW and HD), which transition from the downstream MRB to western mountainous areas. Meanwhile, cold extremes (CW and CD) continue to show highest frequency in the Jiufeng Mountain areas. CCEs under SSP5-8.5 also maintain an increasing trend (0.76d/10a), while SSP2-4.5 shows a slight decreasing tendency (Fig. 5 k–o). Among these events, both wet extremes (CW and HW) show insignificant changes, while HD exhibits an increasing trend (1.18d/10a and 0.46d/10a) and CD displays a decreasing tendency (–0.50d/10a and –0.70d/10a).

Given that precipitation and temperature are crucial climate indicators, we calculate average annual values for both over the MRB and investigate their interannual trends. (Supplement Fig. S2). As shown in Fig. S2, precipitation shows slight variation, maintaining relatively stable annual fluctuations. In contrast, temperature demonstrates marked upward progression, particularly accelerated under high-emission SSP5-8.5 conditions (0.46°C/10a). Therefore, we hypothesize that the variation of CCEs in the MRB is primarily controlled by temperature-driven physical processes (with intensifying hot extremes coinciding with declining cold extremes.). Similar findings are also revealed in earlier research (Wu et al., 2020; Zhao et al., 2024; Duan et al., 2024).

https://doi.org/10.5194/egusphere-2025-2438
Preprint. Discussion started: 16 June 2025


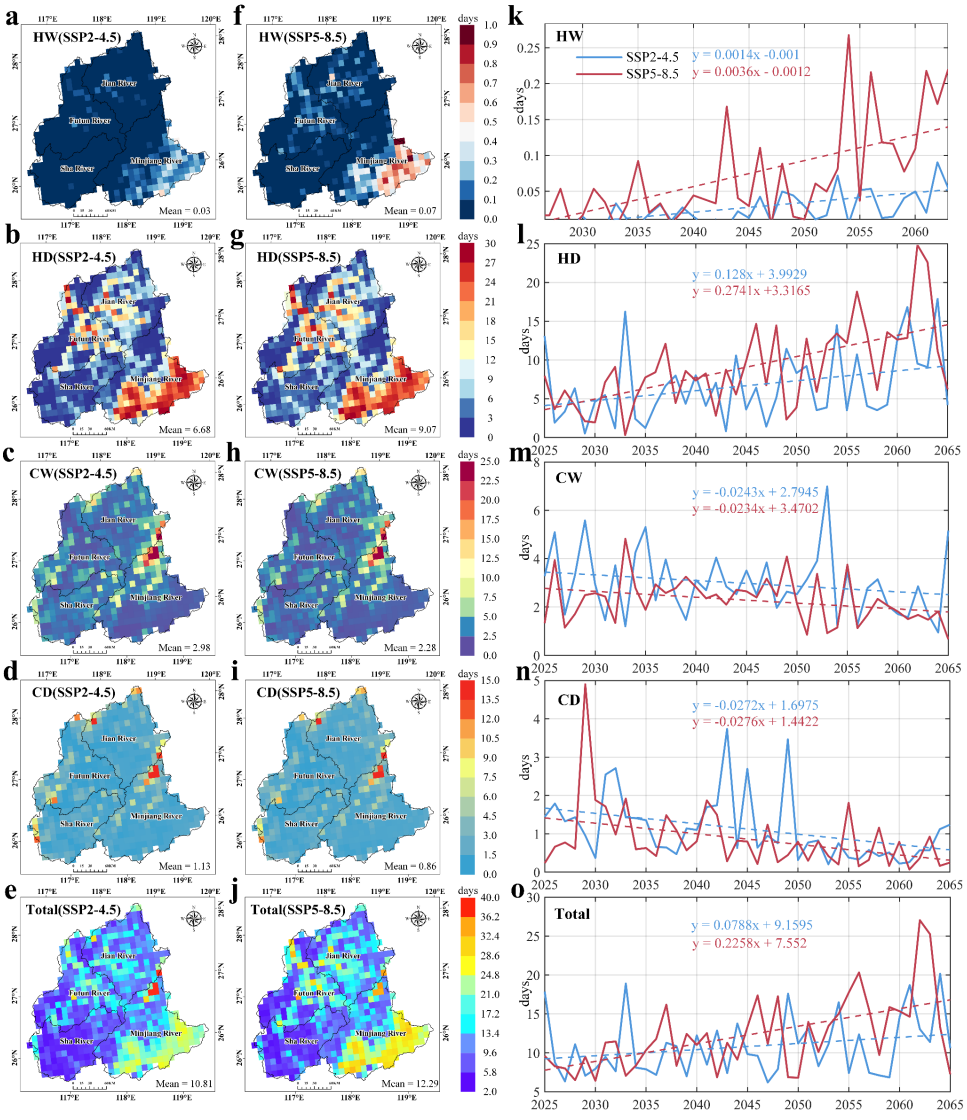


Fig. 4. Same as Fig. 3 but showing results for summer (JJA).

https://doi.org/10.5194/egusphere-2025-2438
Preprint. Discussion started: 16 June 2025


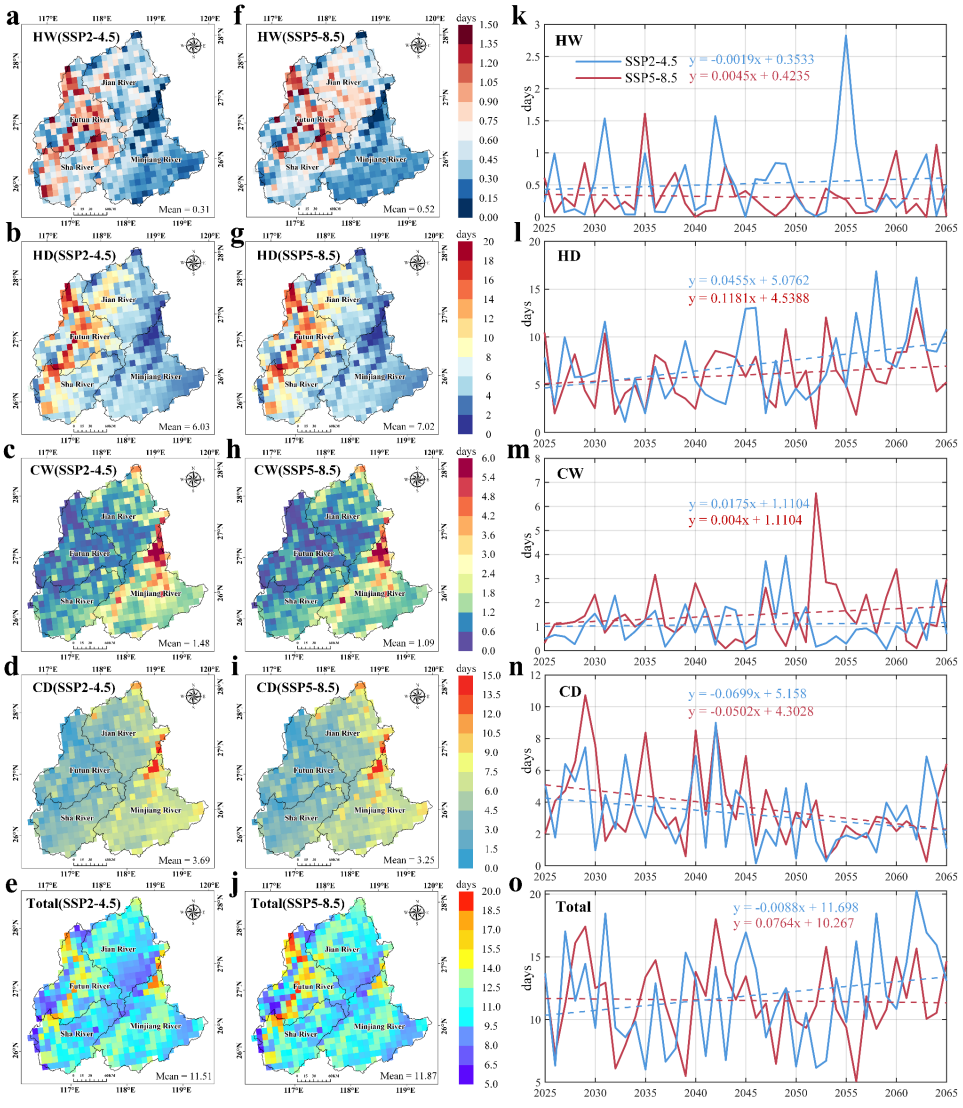


Fig. 5. Same as Fig. 3 but showing results for winter (DJF).

https://doi.org/10.5194/egusphere-2025-2438
Preprint. Discussion started: 16 June 2025


### 3.2 Non-stationary characteristics of CCEs

We examined the variations in both the mean (Mn) and variance (Var) to detect non-stationary characteristics of CCEs (Fig. 6). The GAMLSS model demonstrated excellent fitting performance for all indices except HW, as shown by Filliben coefficients exceeding 0.95 in Fig. S3.

Overall, CCEs exhibit a significant transition from stationary to non-stationary characteristics between SSP2-4.5 and SSP5-8.5 scenarios. This shift is primarily driven by Mn non-stationary changes, which dominated across 80.81% of grid points in the MRB. Additionally, 11.07% of grid points are influenced by combined effects of both Mn and Var, primarily distributed in the Shaxi River Basin and the downstream MRB. Both dry extremes (HD, CD) show a transition from Var to Mn non-stationarity. Specifically, HD's Mn non-stationarity increasing from 22.65% to 57.03% of grids and becoming dominant (60%) in downstream areas where stationarity previously prevailed (54.71%). The Mn non-stationarity of CD also almost covered the entire downstream MRB. For wet extremes (HW and CW), Mn and Var non-stationarity shows a notable increase, with HW expanding from 34.30% to 54.02%, and CW experiencing a stronger rise from 0.06% to 23.25%. In summary, CCEs under SSP5-8.5 demonstrate more pronounced non-stationary characteristics, with dry extremes primarily driven by Mn changes and wet extremes influenced by combined Mn and Var effects.

Figure 7 further illustrates the variations in Mn and Var of CCEs. It is clear that Mn exhibits more pronounced variations compared to Var. For warm extremes, Mn exhibits significant increases across the entire basin under both SSP2-4.5 and SSP5-8.5 scenarios (at the 99% confidence level), indicating that climate warming predominantly amplifies the mean frequency of compound heat extremes rather than their temporal variability. For cold extremes, CD exhibits more pronounced variations compared to CW, and these changes remain predominantly driven by the reduction in Mn. Overall, under the SSP5-8.5 scenario, Mn of CCEs shows a significant increase across nearly the entire basin, while under the SSP2-4.5 scenario, it remains relatively stable. In contrast, Var exhibits only slight changes under both scenarios.

https://doi.org/10.5194/egusphere-2025-2438
Preprint. Discussion started: 16 June 2025


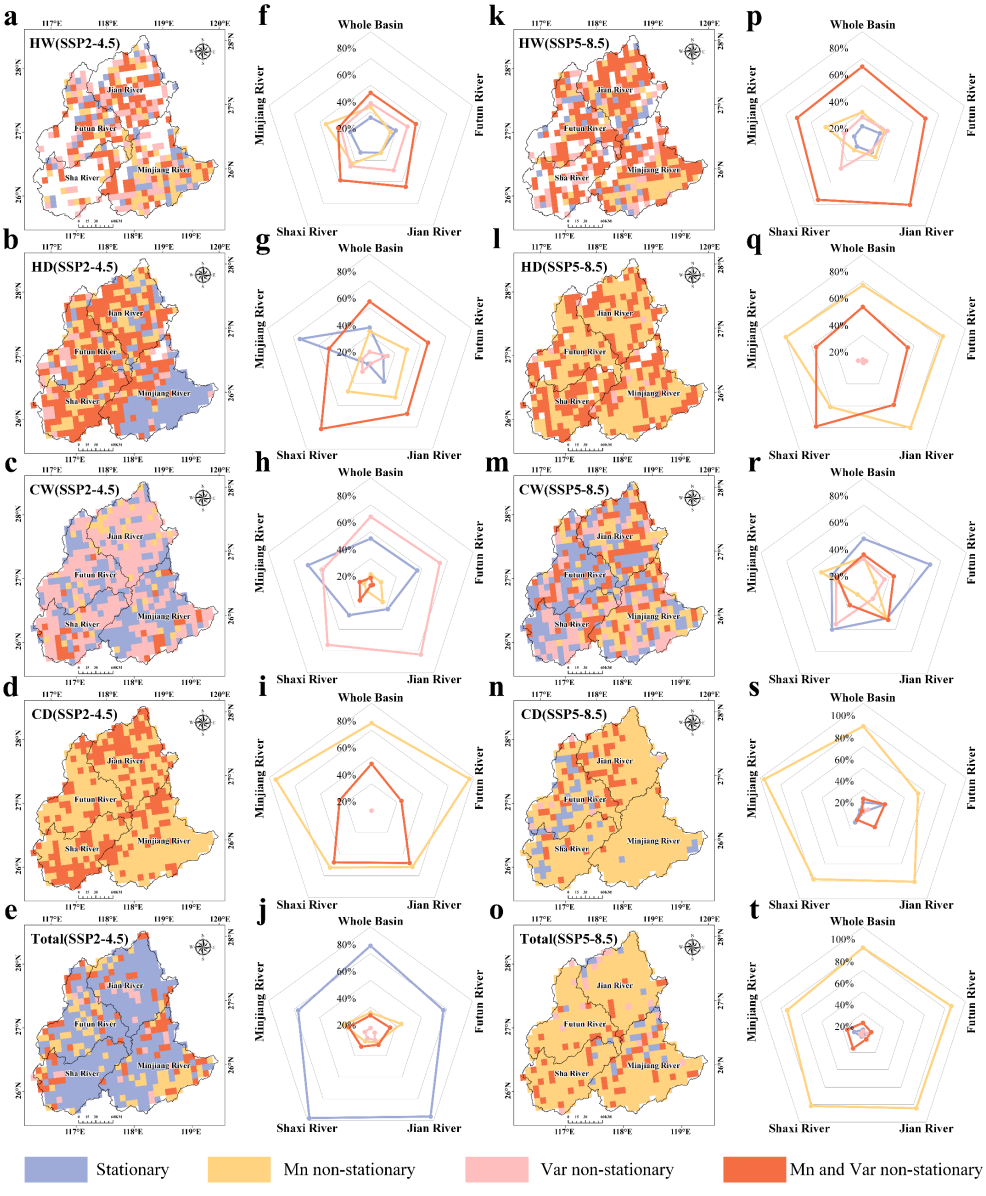


Fig. 6. Stationary and non-stationary characteristics for CCEs in the MRB (a-e and k-o), percentage of non-stationary and stationary characteristics across five basins (f-j and p-t).

https://doi.org/10.5194/egusphere-2025-2438
Preprint. Discussion started: 16 June 2025


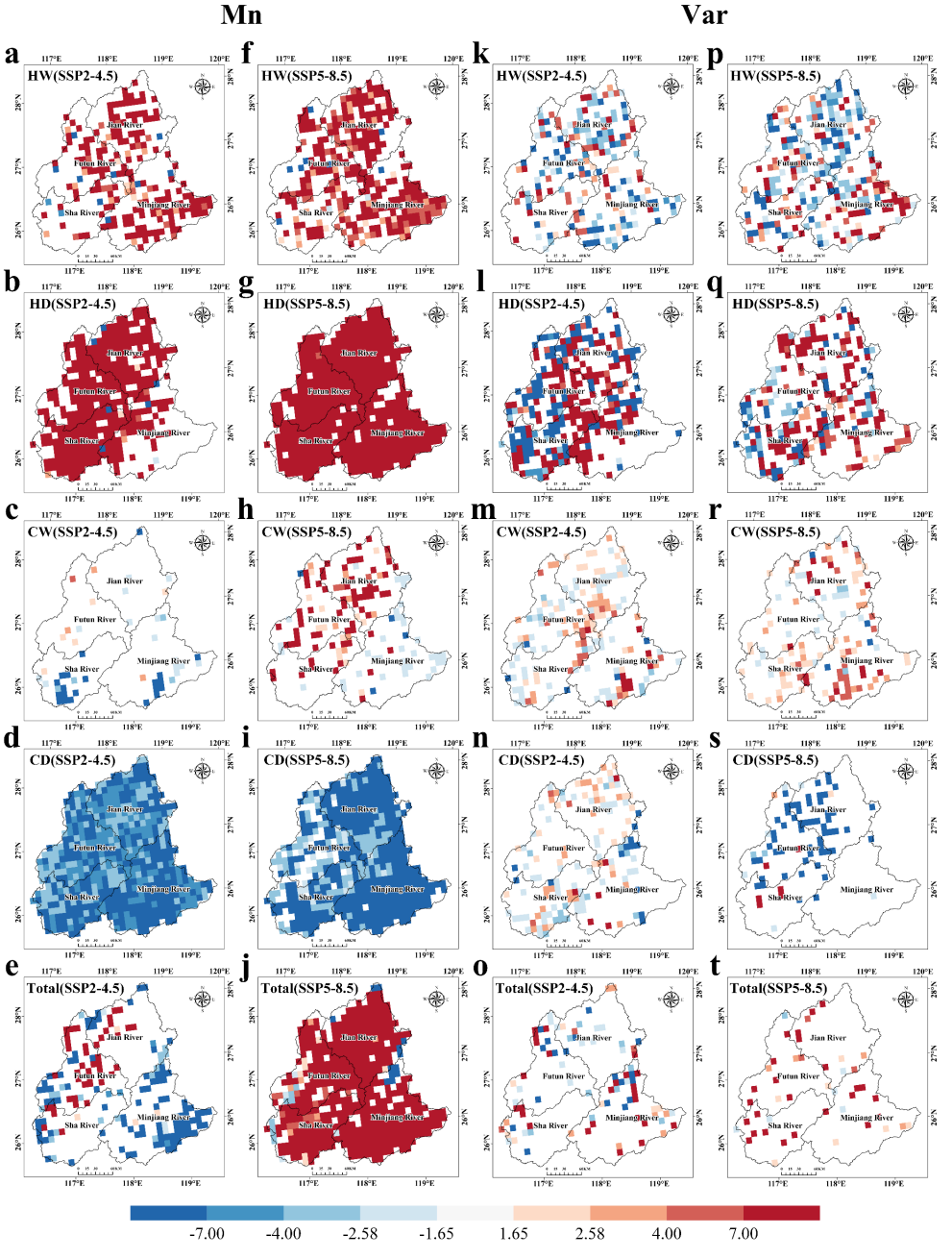


Fig. 7. Results of Mann-Kendall test for Mn (a-j) and Var (k-t), showing the spatial distribution of Z values. Z values indicate trend significance: $|Z| > 1.65$ denotes 90% confidence, while $|Z| > 2.58$ corresponds to 99% confidence.

https://doi.org/10.5194/egusphere-2025-2438
Preprint. Discussion started: 16 June 2025


### 3.3 Changes in the recurrence risks of CCEs

We fit both a non-stationary model and stationary models to investigate the changes in recurrence risk of CCEs. Figure 8 (a-j) presents substantial differences in return period of CCEs under stationary and non-stationary conditions. Our results reveal that stationary models significantly underestimate the recurrence risks of CCEs in future decades, whereas non-stationary models better capture their evolving characteristics. These discrepancies between the two models become more significant over time.

Under the SSP5-8.5 scenario, non-stationary projections show significant increases in the 20-, 50-, and 100-year CCEs. Total CCEs are projected to increase at a rate of 3.12d/10a in 100-year return period. Notably, the stationary models systematically underestimate the risks of CCEs after 2045. Specifically, the recurrence risks of HW (0.36d/10a and 0.15d/10a), HD (11.65d/10a and 2.53d/10a), and CW (0.30d/10a and 0.06d/10a) all show increasing trends, particularly under the SSP5-8.5 scenario. In contrast, CD exhibits a decreasing trend, with a more rapid decline under the SSP2-4.5 scenario (-3.38d/10a). The 100-year CCEs demonstrate higher sensitivity to climate change, highlighting amplified non-stationary effects on these high-impact extremes.

We further quantify the deterministic trends of recurrence risks in CCEs based on the Empirical Mode Decomposition (EMD, Supplement Method S1). Figure 8 k-t present the variations in 100-year recurrence risks, while the complete results for all return periods are provided in Supplement Fig. S4. Overall, CCEs show strong upward trends under the SSP5-8.5 scenario, along with significant spatial heterogeneity. The frequency of CCEs generally shows a decreasing trend from west to east, featuring concentrated high-risk regions in the Shaxi River Basin (some grid points exceed 12d/10a). While all indices except CD show increasing trends, HD emerges as the most severe, with basin-wide increases exceeding 8d/10a. In contrast, CD shows decreasing trends in both scenarios, with a less pronounced decline under SSP5-8.5, suggesting that greenhouse warming has not substantially mitigated recurrence risks associated with CD.

https://doi.org/10.5194/egusphere-2025-2438
Preprint. Discussion started: 16 June 2025


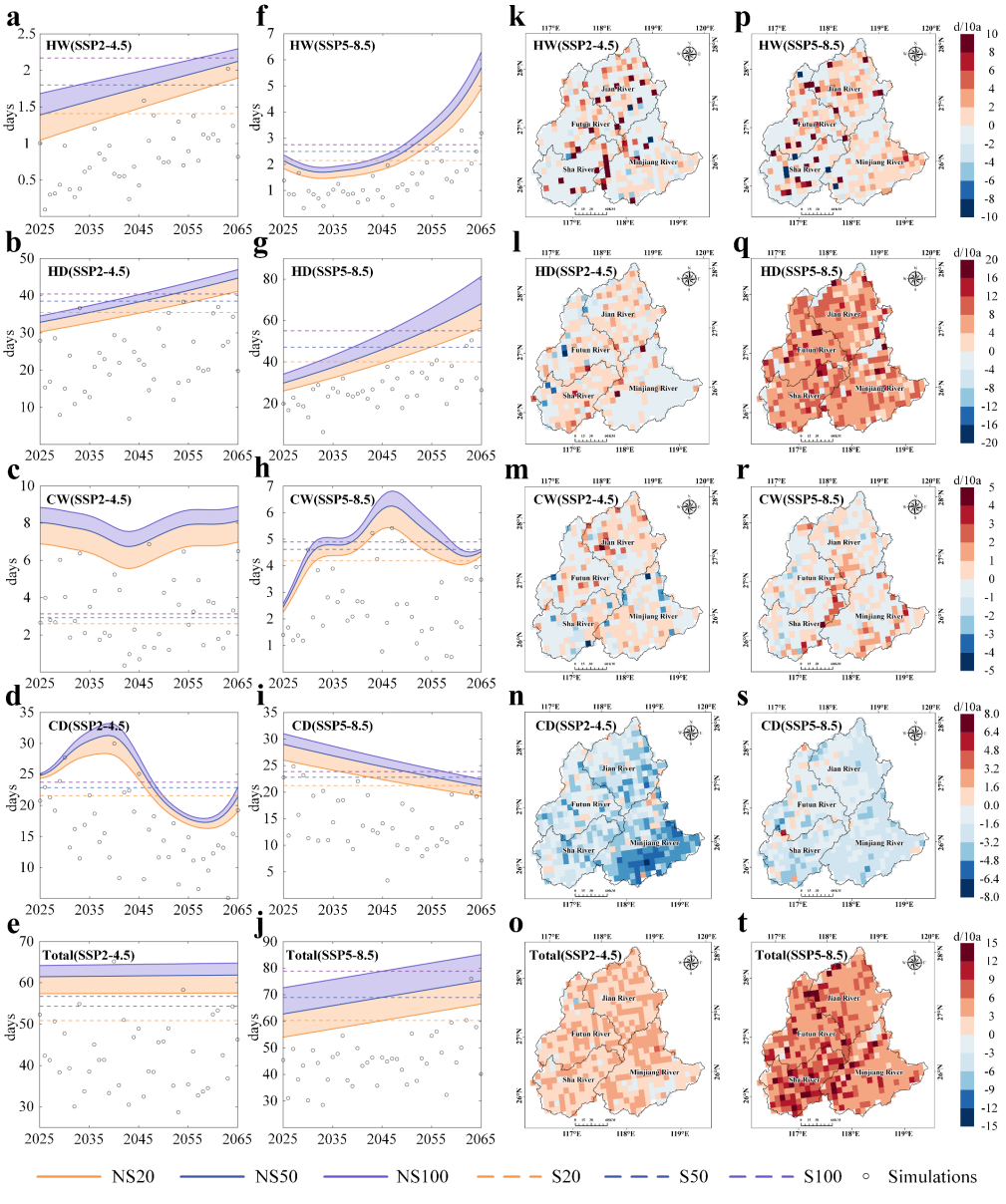


Fig. 8. Comparison of non-stationary (NS) and stationary (S) characteristics for CCEs under 20-, 50-, and 100- year return periods (a-j). Spatial distributions of trends in CCEs under 100-year return periods (k-t), 20- and 50-year return period result are provided in Supplement Fig. S4.

https://doi.org/10.5194/egusphere-2025-2438
Preprint. Discussion started: 16 June 2025


## 4 Discussion

Although earlier research has highlighted the necessity of analyzing extreme events under non-stationary conditions (Cheng et al, 2014; Byun and Hamlet, 2020; Liu et al., 2024), the evolution of CCEs within a non-stationary climate remains lacking. This study develops an innovative non-stationary framework to assess future recurrence risk changes in CCEs, combining WRF with advanced GAMLSS. Our analysis suggests that traditional stationary models may underestimate CCE frequencies. Therefore, updating risk assessments in time under non-stationary conditions is essential to avoid misleading projections and support more robust climate adaptation strategies (Abdelmoaty and Papalexiou, 2023). This innovative framework enables regional-scale reassessment of CCEs which is transferable elsewhere.

The projected increase in CCEs is consistent with global trends of intensifying hydroclimatic risks under continued warming (Asadieh and Krakauer, 2017; Zhang et al., 2021; Shu et al., 2024). Yin et al (2025) indicate that hot-stagnation and hot-dry extremes as the most prevalent CCE types in Eastern Asia, suggesting that temperature variations predominantly influence the occurrence of CCEs in this region. Increasing empirical evidence (Li et al., 2021; Li et al., 2023; Engdaw et al., 2023) reveals that sustained global warming is associated with a rising frequency of hot extremes and a systematic decline in cold extremes. This reversal has been linked to enhanced radiative forcing from anthropogenic greenhouse gas emissions (Samset et al., 2018; Kramer et al., 2021). Our study reveals that future variations in CCEs are predominantly driven by climate warming-induced mean-state shifts rather than enhanced variability. This aligns with global-scale findings that thermodynamic effects (e.g., rising baseline intensity of extremes due to warming) dominate mean-state changes (Horton et al., 2016; Van Der Wiel and Karin, 2021; Nordling et al., 2025). Moreover, conventional stationary models, which rely on fixed statistical assumptions, may fail to capture the escalating severity of future extreme events (Feng et al., 2020; Xu et al., 2025). Our results empirically validate that non-stationary frameworks provide significantly improved estimates of recurrence risk shifts in compound extremes compared to stationary models.

To refine coarse-resolution global climate models (GCMs) outputs, two prevalent downscaling strategies have been established: dynamic and statistical techniques. (Sachindra et al., 2018; Xu et al., 2019). Compared with traditional statistical downscaling approaches, the dynamical

https://doi.org/10.5194/egusphere-2025-2438
Preprint. Discussion started: 16 June 2025


downscaling framework offers significant advantages in representing the physical mechanisms (Gutmann et al., 2011; Guyennon et al., 2013). WRF model is adept at explicitly resolving atmospheric dynamics, surface processes, and land-atmosphere feedback mechanisms (Powers et al., 2017). This capability is especially crucial in the MRB, where complex terrain and significant surface heterogeneity prevail. Furthermore, extensive research confirms that simulation fidelity fundamentally depends on initial and boundary condition quality. (Comin et al., 2018; Gholami et al., 2021; Bello-Millá et al., 2024). Therefore, instead of relying on traditional ensemble prediction, we use bias-corrected CMIP6 dataset, addressing some of the uncertainties at their source. This dataset has also been validated for its reliability (Zhang et al., 2024; Yang et al., 2025; Duan et al., 2025).

Several limitations merit consideration in this study. Firstly, although dynamical downscaling with the WRF model improves spatial resolution, systematic biases remain in precipitation simulations over complex terrain. Secondly, the current GAMLSS framework only considers time as a covariate. Future studies could integrate machine learning approaches for WRF output post-processing (Yin et al., 2021; Xie et al., 2023) while simultaneously incorporating physical covariates (e.g., climate drift, circulation indices) to enhance dynamical modeling frameworks (Zeng et al., 2024; Ma et al., 2025).

## 5 Conclusions

Through this intensive case analysis, we establish a transferable framework for assessing the non-stationarity of CCEs. This work advances the understanding of the evolution of CCE recurrence risks under climate change and offers important perspectives to support adaptive strategies and strengthen disaster risk governance. This study reveals the following important findings.

1) CCEs increase significantly across the MRB, with trends under SSP5-8.5 (3.55d/10a) scenarios surpassing those under SSP2-4.5 scenarios. HD extremes dominate spatially (downstream-focused) and seasonally (summer-peaked), rising at 2.26d/10a, whereas cold extremes decline. These shifts are primarily temperature-driven, as pronounced warming amplifies hot extremes but suppresses cold extremes.
2) CCEs exhibit a pronounced shift toward Mn-dominated non-stationarity under SSP5-8.5

https://doi.org/10.5194/egusphere-2025-2438
Preprint. Discussion started: 16 June 2025


scenarios, contrasting sharply with the stationarity in SSP2-4.5. Spatial analysis reveals that 80.8% of the MRB is governed by Mn-driven non-stationarity under SSP5-8.5, with dry extremes (HD, CD) showing the most abrupt transitions. For HD, Mn non-stationarity expands from 22.7% to 57.0% of the basin, dominating 60% of downstream grids, showing an increase of nearly three times compared to SSP2-4.5. CD's Mn-driven shifts cover >90% of the downstream MRB. Var contributes minimally across both scenarios, confirming that warming amplifies extremes primarily through baseline intensity shifts rather than stochastic fluctuations.

3) Non-stationary modeling reveals systematic underestimation of CCEs recurrence risks by stationary approaches. Under SSP5-8.5 scenarios, most CCEs (except CD) exhibit increasing recurrence risks. Climate change impacts are significantly amplified for 100-year CCEs (3.12d/10a), as evidenced by their heightened non-stationary responses. Spatial analysis reveals a distinct east-to-west gradient in recurrence risk, with significantly elevated risk observed in the western mountainous areas.

**Acknowledgements**

The 'High Performance Computing Center' at Fujian Normal University provided computational resources for the WRF model simulations.

**Financial support**

Supported by the National Natural Science Foundation of China (Grant No. 42271030), Fujian Provincial Funds for Distinguished Young Scientists (Grant No. 2022J06018), the Scientific Project of Fujian Provincial Department of Science and Technology (Grant no. 2022Y0007), the German Federal Ministry of Education and Research (BMBF) through funding of the KARE_II project (01LR2006D1) and the 'Young Eagle Plan' Top Talents of Fujian Province.

**Code/Data availability**

Code/Data will be made available on request.

**Declaration of competing interest**

The authors declare that they have no known competing financial interests or personal relationships that could have appeared to influence the work reported in this paper.

https://doi.org/10.5194/egusphere-2025-2438
Preprint. Discussion started: 16 June 2025


## Author contribution

Conceptualization: YZ. Methodology: YZ, LG, WX, CD, MM, JW, HK. Software: YZ, WX, CD. Data curation: SS. Writing- Original draft preparation: YZ. Writing- Reviewing and Editing: WX, LG. Supervision: SS, MM, YC, HK. Funding acquisition: LG, JW, YC.

## References

Abdelmoaty, H.M., Papalexiou, S.M., 2023. Changes of extreme precipitation in CMIP6 projections: should we use stationary or nonstationary models? J. Climate 36, 2999–3014. https://doi.org/10.1175/JCLI-D-22-0467.1

Abdelmoaty, H.M., Papalexiou, S.M., Rajulapati, C.R., AghaKouchak, A., 2021. Biases beyond the mean in CMIP6 extreme precipitation: A global investigation. Earth's Future 9, e2021EF002196. https://doi.org/10.1029/2021EF002196

Akaike, H., 1974. A new look at the statistical model identification. IEEE T. Automat. Contr. 19(6), 716–723. https://doi.org/10.1109/TAC.1974.1100705

Arakawa, A., Jung, J.-H., 2011. Multiscale modeling of the moist-convective atmosphere — A review. Atmos. Res. 102, 263–285. https://doi.org/10.1016/j.atmosres.2011.08.009

Arnault, J., Jung, G., Haese, B., Fersch, B., Rummler, T., Wei, J., Zhang, Z., Kunstmann, H., 2021. A joint soil-vegetation-atmospheric modeling procedure of water isotopologues: implementation and application to different climate zones with WRF-Hydro-iso. J. Adv. Model Earth Syst. 13. https://doi.org/10.1029/2021MS002562

Asadieh, B., Krakauer, N.Y., 2017. Global change in streamflow extremes under climate change over the 21st century. Hydrol. Earth Syst. Sci. 21, 5863–5874. https://doi.org/10.5194/hess-21-5863-2017

Bello-Millán, F.J., Palacios, J., Gutierrez-Castillo, P., Parras, L., 2024. Simulations of a tornadic supercell event in the south of Spain: Sensitivity to initial and boundary conditions and microphysics parameterizations. Atmos. Res. 300, 107262. https://doi.org/10.1016/j.atmosres.2024.107262

Byun, K., Hamlet, A.F., 2020. A risk-based analytical framework for quantifying non-stationary flood risks and establishing infrastructure design standards in a changing environment. J. Hydrol. 584, 124575. https://doi.org/10.1016/j.jhydrol.2020.124575

https://doi.org/10.5194/egusphere-2025-2438
Preprint. Discussion started: 16 June 2025


390 Chen, S.-H., Sun, W.-Y., 2002. A one-dimensional time dependent cloud model. J. Meteorol. Soc.
391 Japan. 80, 99–118. https://doi.org/10.2151/jmsj.80.99
392 Cheng, L., AghaKouchak, A., Gilleland, E., Katz, R.W., 2014. Non-stationary extreme value
393 analysis in a changing climate. Climatic Change 127, 353–369. https://doi.org/10.1007/s10584-
394 014-1254-5
395 Comin, A.N., Schumacher, V., Justino, F., Fernández, A., 2018. Impact of different microphysical
396 parameterizations on extreme snowfall events in the Southern Andes. Weather Clim. Extremes 21,
397 65–75. https://doi.org/10.1016/j.wace.2018.07.001
398 Croitoru, A.-E., Piticar, A., Ciupertea, A.-F., Roşca, C.F., 2016. Changes in heat waves indices in
399 Romania over the period 1961–2015. Global and Planetary Change 146, 109–121.
400 https://doi.org/10.1016/j.gloplacha.2016.08.016
401 Deng, C., Zhang, Y., Ma, M., Chen, Y., Wei, J., Kunstmann, H., Gao, L., 2025. Compound temporal-
402 spatial extreme precipitation events in the Poyang Lake Basin of China. J. Hydrol.: Reg. Stud. 58,
403 102270. https://doi.org/10.1016/j.ejrh.2025.102270
404 Duan, K., Wang, Q., Yao, T., Wang, N., He, J., Shang, W., Jiang, J., 2025. Glacier evolution model
405 based on physical processes: Application to alpine glacier Laohugou No. 12, Qilian Mountains. Sci.
406 China Earth Sci. https://doi.org/10.1007/s11430-024-1524-8
407 Duan, R., Huang, G., Wang, F., Tian, C., Wu, X., 2024. Observations over a century underscore an
408 increasing likelihood of compound dry-hot events in China. Earth's Future 12, e2024EF004546.
409 https://doi.org/10.1029/2024EF004546
410 Dudhia, J., 1989. Numerical Study of Convection Observed during the Winter Monsoon
411 Experiment Using a Mesoscale Two-Dimensional Model. J. Atmos. Sci. 46, 3077–3107.
412 https://doi.org/10.1175/1520-0469(1989)046<3077:NSOCOD>2.0.CO;2
413 Engdaw, M.M., Steiner, A.K., Hegerl, G.C., Ballinger, A.P., 2023. Attribution of observed changes
414 in extreme temperatures to anthropogenic forcing using CMIP6 models. Weather Clim. Extremes
415 39, 100548. https://doi.org/10.1016/j.wace.2023.100548
416 Feng, J., Qin, T., Lv, X., Liu, S., Wen, J., Chen, J., 2025. Frequent drought and flood events in the
417 Yellow River Basin, increasing future drought trends in the middle and upper reaches. Int. J. Appl.
418 Earth Obs. 139, 104511. https://doi.org/10.1016/j.jag.2025.104511

https://doi.org/10.5194/egusphere-2025-2438
Preprint. Discussion started: 16 June 2025


419 Feng, Y., Shi, P., Qu, S., Mou, S., Chen, C., Dong, F., 2020. Nonstationary flood coincidence risk
420 analysis using time-varying copula functions. Sci. Rep. 10, 3395. https://doi.org/10.1038/s41598-
421 020-60264-3
422 Filliben, J.J., 1975. The probability plot correlation coefficient test for normality. Technometrics 17,
423 111–117. https://doi.org/10.1080/00401706.1975.10489279
424 Gao, L., Huang, J., Chen, X., Chen, Y., Liu, M., 2018. Contributions of natural climate changes and
425 human activities to the trend of extreme precipitation. Atmos. Res. 205, 60–69.
426 https://doi.org/10.1016/j.atmosres.2018.02.006
427 Gholami, S., Ghader, S., Khaleghi-Zavareh, H., Ghafarian, P., 2021. Sensitivity of WRF-simulated
428 10 m wind over the Persian Gulf to different boundary conditions and PBL parameterization
429 schemes. Atmos. Res. 247, 105147. https://doi.org/10.1016/j.atmosres.2020.105147
430 Gutmann, E.D., Rasmussen, R.M., Liu, C., Ikeda, K., Gochis, D.J., Clark, M.P., Dudhia, J.,
431 Thompson, G., 2012. A Comparison of Statistical and Dynamical Downscaling of Winter
432 Precipitation over Complex Terrain. J. Climate 25, 262–281.
433 https://doi.org/10.1175/2011JCLI4109.1
434 Guyennon, N., Romano, E., Portoghese, I., Salerno, F., Calmanti, S., Petrangeli, A.B., Tartari, G.,
435 Copetti, D., 2013. Benefits from using combined dynamical-statistical downscaling approaches –
436 lessons from a case study in the Mediterranean region. Hydrol. Earth Syst. Sci. 17, 705–720.
437 https://doi.org/10.5194/hess-17-705-2013
438 Hong, S.-Y., Noh, Y., Dudhia, J., 2006. A New Vertical Diffusion Package with an Explicit
439 Treatment of Entrainment Processes. Mon. Weather Rev. 134, 2318–2341.
440 https://doi.org/10.1175/MWR3199.1
441 Horton, R.M., Mankin, J.S., Lesk, C., Coffel, E., Raymond, C., 2016. A Review of Recent Advances
442 in Research on Extreme Heat Events. Curr. Clim. Change Rep. 2, 242–259.
443 https://doi.org/10.1007/s40641-016-0042-x
444 Huang, N.E., Shen, Z., Long, S.R., Wu, M.C., Shih, H.H., Zheng, Q., Yen, N.-C., Tung, C.C., Liu,
445 H.H., 1998. The empirical mode decomposition and the Hilbert spectrum for nonlinear and non-
446 stationary time series analysis. Proc. R. Soc. Lond. A. 454, 903–995.
447 https://doi.org/10.1098/rspa.1998.0193

https://doi.org/10.5194/egusphere-2025-2438
Preprint. Discussion started: 16 June 2025


448 IPCC, 2021. Weather and climate extreme events in a changing climate. In climate change 2021:
449 The physical science basis. Contribution of Working Group I to the Sixth Assessment Report of the
450 Intergovernmental Panel on Climate Change. Cambridge University Press, Cambridge, United
451 Kingdom and New York, NY, USA, pp. 1513–1766, https://doi: 10.1017/9781009157896.013.
452 Jia, N., Cheng, J., Li, Y., Zheng, L., Song, W., Chen, R., Zhu, A., 2025. China's Yangtze River
453 drought: A cascade of impacts from mountains to sea. Sci. China Earth Sci. 68, 957–962.
454 https://doi.org/10.1007/s11430-024-1521-3
455 Jiang, Q., Li, W., Fan, Z., He, X., Sun, W., Chen, S., Wen, J., Gao, J., Wang, J., 2021. Evaluation of
456 the ERA5 reanalysis precipitation dataset over Chinese Mainland. J. Hydrol. 595, 125660.
457 https://doi.org/10.1016/j.jhydrol.2020.125660
458 Jin, H., Willems, P., Chen, X., Liu, M., 2023. Nonstationary flood and its influencing factors
459 analysis in the Hanjiang River Basin, China. J. Hydrol. 625, 129994.
460 https://doi.org/10.1016/j.jhydrol.2023.129994
461 Kim, Y.-H., Min, S.-K., Zhang, X., Sillmann, J., Sandstad, M., 2020. Evaluation of the CMIP6
462 multi-model ensemble for climate extreme indices. Weather Clim. Extremes 29, 100269.
463 https://doi.org/10.1016/j.wace.2020.100269
464 Kramer, R.J., He, H., Soden, B.J., Oreopoulos, L., Myhre, G., Forster, P.M., Smith, C.J., 2021.
465 Observational evidence of increasing global radiative forcing. Geophys. Res. Lett. 48,
466 e2020GL091585. https://doi.org/10.1029/2020GL091585
467 Lee, T., Ouarda, T.B.M.J., 2010. Long-term prediction of precipitation and hydrologic extremes
468 with nonstationary oscillation processes. J. Geophys. Res. 115, 2009JD012801.
469 https://doi.org/10.1029/2009JD012801
470 Lei, X., Gao, L., Ma, M., Wei, J., Xu, L., Wang, L., Lin, H., 2021. Does non-stationarity of extreme
471 precipitation exist in the Poyang Lake Basin of China? J. Hydrol.: Reg. Stud. 37, 100920.
472 https://doi.org/10.1016/j.ejrh.2021.100920
473 Li, C., Zwiers, F., Zhang, X., Li, G., Sun, Y., Wehner, M., 2021. Changes in annual extremes of
474 daily temperature and precipitation in CMIP6 models. J. Climate 34, 3441–3460.
475 https://doi.org/10.1175/JCLI-D-19-1013.1
476 Li, M., Feng, Z., Zhang, M., Yao, Y., 2024. Influence of large-scale climate indices and regional

https://doi.org/10.5194/egusphere-2025-2438
Preprint. Discussion started: 16 June 2025


meteorological elements on drought characteristics in the Luanhe River Basin. Atmos. Res. 300, 107219. https://doi.org/10.1016/j.atmosres.2024.107219

Li, Y., Ren, G., Wang, Q., Mu, L., 2023. Changes in marine hot and cold extremes in the China Seas during 1982–2020. Weather Clim. Extremes 39, 100553. https://doi.org/10.1016/j.wace.2023.100553

Lin, S., Zhang, Y., Sun, S., Guan, X., Jiang, C., Gao, L., 2023. Sensitivity study of WRF parameterization schemes and initial fields on simulation of rainstorm in the Minjiang River basin. Pearl River (in Chinese) 44(10):35-46+61. https://doi: 10.3969/j.issn.1001-9235.2023.10.004

Liu, H., Xiao, P., Zhang, X., Liang, Y., Tang, B., Chen, S., Liu, Y., 2024. Winter snowpack loss increases warm-season compound hot-dry extremes. Commun. Earth Environ. 5, 567. https://doi.org/10.1038/s43247-024-01734-8

Liu, Y., Chen, J., Xiong, L., Xu, C.-Y., 2024. Integrating heterogeneous information for modeling non-stationarity of extreme precipitation in the Yangtze River Basin. J. Hydrol. 645, 132159. https://doi.org/10.1016/j.jhydrol.2024.132159

Ma, L., Hu, S., Zhou, B., Peng, J., Li, D., 2025. Novel dynamical indices for the variations of the South Asia high in a warming climate. Atmos. Res. 315, 107901. https://doi.org/10.1016/j.atmosres.2024.107901

Mlawer, E.J., Taubman, S.J., Brown, P.D., Iacono, M.J., Clough, S.A., 1997. Radiative transfer for inhomogeneous atmospheres: RRTM, a validated correlated-k model for the longwave. J. Geophys. Res.: Atmos. 102, 16663–16682. https://doi.org/10.1029/97JD00237

Miao, L., Ju, L., Sun, S., Agathokleous, E., Wang, Q., Zhu, Z., Liu, R., Zou, Y., Lu, Y., Liu, Q., 2024. Unveiling the dynamics of sequential extreme precipitation-heatwave compounds in China. npj Clim. Atmos. Sci. 7, 67. https://doi.org/10.1038/s41612-024-00613-5

Mukherjee, S., Mishra, A.K., Zscheischler, J., Entekhabi, D., 2023. Interaction between dry and hot extremes at a global scale using a cascade modeling framework. Nat. Commun. 14, 277. https://doi.org/10.1038/s41467-022-35748-7

Nerantzaki, S.D., Papalexiou, S.M., Rajulapati, C.R., Clark, M.P., 2023. Nonstationarity in high and low-temperature extremes: Insights from a global observational data set by merging extreme-value methods. Earth's Future 11, e2023EF003506. https://doi.org/10.1029/2023EF003506

https://doi.org/10.5194/egusphere-2025-2438
Preprint. Discussion started: 16 June 2025


506 Niu, G.-Y., Yang, Z.-L., Mitchell, K.E., Chen, F., Ek, M.B., Barlage, M., Kumar, A., Manning, K.,
507 Niyogi, D., Rosero, E., Tewari, M., Xia, Y., 2011. The community Noah land surface model with
508 multiparameterization options (Noah-MP): 1. Model description and evaluation with local-scale
509 measurements. J. Geophys. Res.: Atmos. 116, D12109. https://doi.org/10.1029/2010JD015139
510 Nordling, K., Fahrenbach, N.L.S., Samset, B.H., 2025. Climate variability can outweigh the
511 influence of climate mean changes for extreme precipitation under global warming. Atmos. Chem.
512 Phys. 25, 1659–1684. https://doi.org/10.5194/acp-25-1659-2025
513 Patel, R.N., Bonan, D.B., Schneider, T., 2024. Changes in the frequency of observed temperature
514 extremes largely driven by a distribution shift. Geophys. Res. Lett. 51, e2024GL110707.
515 https://doi.org/10.1029/2024GL110707
516 Powers, J.G., Klemp, J.B., Skamarock, W.C., Davis, C.A., Dudhia, J., Gill, D.O., Coen, J.L., Gochis,
517 D.J., Ahmadov, R., Peckham, S.E., Grell, G.A., Michalakes, J., Trahan, S., Benjamin, S.G.,
518 Alexander, C.R., Dimego, G.J., Wang, W., Schwartz, C.S., Romine, G.S., Liu, Z., Snyder, C., Chen,
519 F., Barlage, M.J., Yu, W., Duda, M.G., 2017. The Weather Research and Forecasting Model:
520 Overview, System Efforts, and Future Directions. B. Am. Meteorol. Soc. 98, 1717–1737.
521 https://doi.org/10.1175/BAMS-D-15-00308.1
522 Qian, C., 2016. On trend estimation and significance testing for non-Gaussian and serially
523 dependent data: quantifying the urbanization effect on trends in hot extremes in the megacity of
524 Shanghai. Clim. Dyn. 47, 329–344. https://doi.org/10.1007/s00382-015-2838-0
525 Rahimi, S., Huang, L., Norris, J., Hall, A., Goldenson, N., Risser, M., Feldman, D.R., Lebo, Z.J.,
526 Dennis, E., Thackeray, C., 2024. Understanding the cascade: removing GCM biases improves
527 dynamically downscaled climate projections. Geophys. Res. Lett. 51, e2023GL106264.
528 https://doi.org/10.1029/2023GL106264
529 Rigby, R.A., Stasinopoulos, D.M., 2005. Generalized dditive Models for Location, Scale and Shape.
530 J. R. Stat. Soc. C-Appl. 54, 507–554. https://doi.org/10.1111/j.1467-9876.2005.00510.x
531 Sachindra, D.A., Ahmed, K., Rashid, Md.M., Shahid, S., Perera, B.J.C., 2018. Statistical
532 downscaling of precipitation using machine learning techniques. Atmos. Res. 212, 240–258.
533 https://doi.org/10.1016/j.atmosres.2018.05.022
534 Saini, R., Attada, R., 2025. Indian summer monsoon precipitation and extremes over the Indian

https://doi.org/10.5194/egusphere-2025-2438
Preprint. Discussion started: 16 June 2025


Himalayas in WRF dynamically downscaled (HARv2) reanalysis. Clim. Dyn. 63, 158. https://doi.org/10.1007/s00382-025-07648-1

Samset, B.H., Sand, M., Smith, C.J., Bauer, S.E., Forster, P.M., Fuglestvedt, J.S., Osprey, S., Schleussner, C. -F., 2018. Climate impacts from a removal of anthropogenic aerosol emissions. Geophys. Res. Lett. 45, 1020–1029. https://doi.org/10.1002/2017GL076079

Sauter, C., Fowler, H.J., Westra, S., Ali, H., Peleg, N., White, C.J., 2023. Compound extreme hourly rainfall preconditioned by heatwaves most likely in the mid-latitudes. Weather Clim. Extremes 40, 100563. https://doi.org/10.1016/j.wace.2023.100563

Shang, S., Arnault, J., Zhu, G., Chen, H., Wei, J., Zhang, K., Zhang, Z., Laux, P., Kunstmann, H., 2022. Recent increase of spring precipitation over the three-river headwaters region—water budget analysis based on global reanalysis (ERA5) and ET-tagging extended regional climate modeling. J. Climate 35, 7199–7217. https://doi.org/10.1175/JCLI-D-21-0829.1

Shao, S., Zhang, H., Singh, V.P., Ding, H., Zhang, J., Wu, Y., 2022. Nonstationary analysis of hydrological drought index in a coupled human-water system: Application of the GAMLSS with meteorological and anthropogenic covariates in the Wuding River basin, China. J. Hydrol. 608, 127692. https://doi.org/10.1016/j.jhydrol.2022.127692

Shu, Z., Jin, J., Zhang, J., Wang, G., Lian, Y., Liu, Y., Bao, Z., Guan, T., He, R., Liu, C., Jing, P., 2024. 1.5℃ and 2.0℃ of global warming intensifies the hydrological extremes in China. J. Hydrol. 635, 131229. https://doi.org/10.1016/j.jhydrol.2024.131229

Singh, D., Vardhan, M., Sahu, R., Chatterjee, D., Chauhan, P., Liu, S., 2023. Machine-learning- and deep-learning-based streamflow prediction in a hilly catchment for future scenarios using CMIP6 GCM data. Hydrol. Earth Syst. Sci. 27, 1047–1075. https://doi.org/10.5194/hess-27-1047-2023

Song, X., Zhang, J., Zou, X., Zhang, C., AghaKouchak, A., Kong, F., 2019. Changes in precipitation extremes in the Beijing metropolitan area during 1960–2012. Atmos. Res. 222, 134–153. https://doi.org/10.1016/j.atmosres.2019.02.006

Stasinopoulos, D.M., Rigby, R.A., 2007. Generalized Additive Models for Location Scale and Shape (GAMLSS) in R. J. Stat. Soft. 23. https://doi.org/10.18637/jss.v023.i07

Sun, F., Roderick, M.L., Farquhar, G.D., 2018. Rainfall statistics, stationarity, and climate change. Proc. Natl. Acad. Sci. U.S.A. 115, 2305–2310. https://doi.org/10.1073/pnas.1705349115

https://doi.org/10.5194/egusphere-2025-2438
Preprint. Discussion started: 16 June 2025


564 Talbot, C., Bou-Zeid, E., Smith, J., 2012. Nested mesoscale large-eddy simulations with WRF:
565 performance in real test cases. J. Hydrometeorol. 13, 1421–1441. https://doi.org/10.1175/JHM-D-
566 11-048.1
567 Tapiador, F.J., Navarro, A., Moreno, R., Sánchez, J.L., García-Ortega, E., 2020. Regional climate
568 models: 30 years of dynamical downscaling. Atmos. Res. 235, 104785.
569 https://doi.org/10.1016/j.atmosres.2019.104785
570 Van Der Wiel, K., Bintanja, R., 2021. Contribution of climatic changes in mean and variability to
571 monthly temperature and precipitation extremes. Commun. Earth Environ. 2, 1.
572 https://doi.org/10.1038/s43247-020-00077-4
573 Varga, Á.J., Breuer, H., 2022. Evaluation of convective parameters derived from pressure level and
574 native ERA5 data and different resolution WRF climate simulations over Central Europe. Clim.
575 Dyn. 58, 1569–1585. https://doi.org/10.1007/s00382-021-05979-3
576 Wu, J., Wang, Z., Dong, J., Cui, X., Tao, S., Chen, X., 2023. Robust runoff prediction with
577 explainable artificial intelligence and meteorological variables from deep learning ensemble model.
578 Water Resour. Res. 59, e2023WR035676. https://doi.org/10.1029/2023WR035676
579 Wu, X., Hao, Z., Zhang, X., Li, C., Hao, F., 2020. Evaluation of severity changes of compound dry
580 and hot events in China based on a multivariate multi-index approach. J. Hydrol. 583, 124580.
581 https://doi.org/10.1016/j.jhydrol.2020.124580
582 Wu, Y., Miao, C., Slater, L., Fan, X., Chai, Y., Sorooshian, S., 2024. Hydrological projections under
583 CMIP5 and CMIP6: sources and magnitudes of uncertainty. B. Am. Meteorol. Soc. 105, E59–E74.
584 https://doi.org/10.1175/BAMS-D-23-0104.1
585 Wu, Y., Miao, C., Sun, Y., AghaKouchak, A., Shen, C., Fan, X., 2021. Global observations and
586 CMIP6 simulations of compound extremes of monthly temperature and precipitation. GeoHealth 5,
587 e2021GH000390. https://doi.org/10.1029/2021GH000390
588 Xie, Y., Sun, W., Ren, M., Chen, S., Huang, Z., Pan, X., 2023. Stacking ensemble learning models
589 for daily runoff prediction using 1D and 2D CNNs. Expert Syst. Appl. 217, 119469.
590 https://doi.org/10.1016/j.eswa.2022.119469
591 Xu, W., Liu, Z., Gao, L., Lei, X., Zhang, Y., 2025. Changes in Global Marine Heatwaves in a Non-
592 stationary Climate. Geophys. Res. Lett. 52, e2024GL114497.

https://doi.org/10.5194/egusphere-2025-2438
Preprint. Discussion started: 16 June 2025


https://doi.org/10.1029/2024GL114497

Xu, Z., Han, Y., Yang, Z., 2019. Dynamical downscaling of regional climate: A review of methods and limitations. Sci. China Earth Sci. 62, 365–375. https://doi.org/10.1007/s11430-018-9261-5

Xu, Z., Han, Y., Tam, C.-Y., Yang, Z.-L., Fu, C., 2021. Bias-corrected CMIP6 global dataset for dynamical downscaling of the historical and future climate (1979–2100). Sci. Data 8, 293. https://doi.org/10.1038/s41597-021-01079-3

Yang, T., Chen, X., Hamdi, R., Li, L., Cui, F., De Maeyer, P., Duan, W., 2025. Rainfall-Driven Extreme Snowmelt Will Increase in the Tianshan and Pamir Regions Under Future Climate Projection. J. Geophys. Res.: Atmos. 130, e2024JD042323. https://doi.org/10.1029/2024JD042323

Yin, C., Ting, M., Kornhuber, K., Horton, R.M., Yang, Y., Jiang, Y., 2025. CETD, a global compound events detection and visualisation toolbox and dataset. Sci. Data 12, 356. https://doi.org/10.1038/s41597-025-04530-x

Yin, H., Zhang, X., Wang, F., Zhang, Y., Xia, R., Jin, J., 2021. Rainfall-runoff modeling using LSTM-based multi-state-vector sequence-to-sequence model. J. Hydrol. 598, 126378. https://doi.org/10.1016/j.jhydrol.2021.126378

You, J., Wang, S., Zhang, B., 2024. Spatially seamless and temporally continuous assessment on compound flood risk in Hong Kong. J. Hydrol. 645, 132217. https://doi.org/10.1016/j.jhydrol.2024.132217

You, J., Yin, F., Gao, L., 2025. Escalating wind power shortages during heatwaves. Commun. Earth Environ. 6, 245. https://doi.org/10.1038/s43247-025-02239-8

Yuan, S., Liu, Yongqiang, Liu, Yongnan, Zhang, K., Li, Yongkang, Enwer, R., Li, Yaqian, Hu, Q., 2024. Spatiotemporal variations of surface albedo in Central Asia and its influencing factors and confirmatory path analysis during the 21st century. Int. J. Appl. Earth Obs. 134, 104233. https://doi.org/10.1016/j.jag.2024.104233

Zeng, J., Li, H., Sun, B., Chen, H., Wang, H., Zhou, B., Duan, M., 2024. Summertime compound heat wave and drought events in China: interregional and subseasonal characteristics, and the associated driving factors. Environ. Res. Lett. 19, 074046. https://doi.org/10.1088/1748-9326/ad5576

Zeng, J., Zhang, S., Zhou, S., Obulkasim, O., Zhang, H., Lu, X., Dai, Y., 2024. Comparison of the

https://doi.org/10.5194/egusphere-2025-2438
Preprint. Discussion started: 16 June 2025


risks and drivers of compound hot-dry and hot-wet extremes in a warming world. Environ. Res. Lett. 19, 114026. https://doi.org/10.1088/1748-9326/ad7617

Zhang, B., Chen, Y., Chen, X., Gao, L., Deng, H., Liu, M., 2024. Effectiveness and resilience of BMPs to watershed climate adaptation considering the uncertainty of hydrological model and GCMs. Clim. Risk Manag. 44, 100612. https://doi.org/10.1016/j.crm.2024.100612

Zhang, C., Wang, Y., Hamilton, K., 2011. Improved Representation of Boundary Layer Clouds over the Southeast Pacific in ARW-WRF Using a Modified Tiedtke Cumulus Parameterization Scheme*. Mon. Weather Rev. 139, 3489–3513. https://doi.org/10.1175/MWR-D-10-05091.1

Zhang, J., Zhao, T., Zhang, Juanjuan, Ren, Y., Li, Z., 2024. Changes in compound temperature and precipitation extremes from combined effects of multiple circulation factors over China. J. Hydrol. 642, 131884. https://doi.org/10.1016/j.jhydrol.2024.131884

Zhang, L., Zhao, Y., Cheng, T.F., Lu, M., 2024. Future changes in global atmospheric rivers projected by CMIP6 models. J. Geophys. Res.: Atmos. 129, e2023JD039359. https://doi.org/10.1029/2023JD039359

Zhang, M., Han, Y., Xu, Z., Guo, W., 2024. Assessing Climate Extremes in Dynamical Downscaling Simulations Driven by a Novel Bias - Corrected CMIP6 Data. J. Geophys. Res.: Atmos. 129, e2024JD041253. https://doi.org/10.1029/2024JD041253

Zhang, W., Furtado, K., Wu, P., Zhou, T., Chadwick, R., Marzin, C., Rostron, J., Sexton, D., 2021. Increasing precipitation variability on daily-to-multiyear time scales in a warmer world. Sci. Adv. 7, eabf8021. https://doi.org/10.1126/sciadv.abf802

Zhang, Y., Deng, C., Xu, W., Zhuang, Y., Jiang, L., Jiang, C., Guan, X., Wei, J., Ma, M., Chen, Y., Peng, J., Gao, L., 2025. Long-term variability of extreme precipitation with WRF model at a complex terrain River Basin. Sci. Rep. 15, 156. https://doi.org/10.1038/s41598-024-84076-x

Zhao, T., Xiong, S., Tian, Y., Wu, Y., Li, B., Chen, X., 2024. Compound dry and hot events over major river basins of the world from 1921 to 2020. Weather Clim. Extremes 44, 100679. https://doi.org/10.1016/j.wace.2024.100679

Zheng, M., Chen, X., Ruan, W., Yao, H., Gu, Z., Geng, K., Li, X., Deng, H., Chen, Y., Liu, M., 2023. Spatiotemporal variation of water cycle components in Minjiang River Basin based on a correction method for evapotranspiration products. J. Hydrol.: Reg. Stud. 50, 101575.

https://doi.org/10.5194/egusphere-2025-2438
Preprint. Discussion started: 16 June 2025


651 https://doi.org/10.1016/j.ejrh.2023.101575